*Article*

# Maximum Doppler Shift Identification Using Decision Feedback Channel Estimation

Yudai Handa, Hiroya Hayakawa, Riku Tanaka, Kosuke Tamura [ID], Jaesang Cha *[ID] and Chang-Jun Ahn [ID]

Graduate School of Engineering, Chiba University, Chiba 263-8522, Japan;
24wm4330@student.gs.chiba-u.jp (Y.H.); junny@faculty.chiba-u.jp (C.-J.A.)
* Correspondence: chajaesang@gmail.com

**Abstract:** This paper introduces a new method for estimating the maximum Doppler shift using decision feedback channel estimation (DFCE). In highly mobile environments, which are expected to be covered beyond 5G and 6G systems, the relative movement between the transmitter and receiver causes Doppler shifts. This leads to inter-carrier interference (ICI), significantly degrading communication quality. To mitigate this effect, systems that estimate the maximum Doppler shift and adaptively adjust communication parameters have been extensively studied. One of the most promising methods for maximum Doppler shift estimation involves inserting pilot signals at both the beginning and end of the packet. Although this method achieves high estimation accuracy, it introduces significant latency due to the insertion of the pilot signal at the packet's end. To address this issue, this paper proposes a new method for rapid estimation using DFCE. The proposed approach compensates for faded signals using channel state information obtained from decision feedback. By treating the compensated signal as a reference, the Doppler shift can be accurately estimated without the need for pilot signals at the end of the packet. This method not only maintains high estimation accuracy but also significantly reduces the latency associated with conventional techniques, making it well-suited for the requirements of next-generation communication systems.

**Keywords:** beyond 5G; 6G; Doppler shift; decision feedback channel estimation (DFCE)

## 1. Introduction

The widespread adoption of wireless mobile communication devices, including the massive proliferation of mobile phones and the Internet of Things (IoT), has resulted in a dramatic surge in data traffic—a trend that shows no signs of slowing down [1,2]. This escalating demand is pushing the boundaries of current communication technologies, necessitating the development of next-generation systems, specifically beyond 5G and 6G. These advanced technologies are designed to meet six key requirements: ultra-high-speed communications, ultra-low latency, ultra-wide range coverage, ultra-low power consumption, ultra-reliable communications, and ultra-multiplexing with integrated sensing capabilities [3,4]. Beyond 5G and 6G technologies are poised to support cutting-edge applications such as V2X (vehicle-to-everything) communications and LEO (low Earth orbit) satellite networks, which demand both scalability across numerous communication systems and minimal latency [5,6].

One of the key challenges in advanced communication systems, symbolized by Beyond 5G and 6G, is signal distortion due to the Doppler shift caused by the relative movement of the transmitter and receiver. In stationary communication scenarios with little or no mobility, the signal is typically subject to reflection and diffraction, leading to frequency-selective fading. In these cases, the channel impulse response remains relatively stable over time, and the channel exhibits long coherence times. However, in high-mobility scenarios, such as vehicular and satellite communications, the rapid movement of communication nodes causes the signal to experience both frequency and time selectivity. This movement

induces a Doppler shift in the carrier frequency, creating an environment characterized by double selectivity. Signals affected by double selectivity undergo significant distortion, which can severely degrade communication quality [7]. In this paper, a coherent scheme is assumed. A coherent scheme is communication by understanding the phase information of signals. In this scheme, we can use both amplitude and phase information of the signals, which can lead to improved signal-to-noise ratio (SNR) and higher efficiency. However, it is vulnerable to phase changes, which can lead to serious errors in high mobile communication environments [8]. To mitigate these effects and maintain reliable communication, strategies that adaptively adjust communication parameters, such as adaptive modulation (AM), are crucial [9].

The strategy of adaptive communication parameter control adjusts parameters based on real-time assessments of the communication environment, such as SNR, K-factor, and Doppler shift [10,11]. For instance, in adaptive modulation (AM), the modulation order is adjusted according to the communication conditions—switching to higher-speed communication in favorable environments and ensuring reliable communication in challenging conditions. This dynamic adjustment helps reduce packet retransmissions and improve communication efficiency. Additionally, power allocation strategies enhance overall throughput by adjusting power distribution based on the communication environment. In high-mobility environments, the most critical factor for adaptive control is the Doppler shift. Therefore, accurate estimation of the Doppler shift and timely feedback to the entire system is essential for maintaining optimal performance in next-generation communication systems designed to operate in highly mobile environments.

A related study outlines conventional methods for estimating the maximum Doppler shift. One promising conventional method involves placing pilot signals at both the beginning and end of a packet. This approach estimates the maximum Doppler shift and the speed of the mobile by calculating the difference between the signals and sorting the data based on a threshold derived from the phase difference in the channel state information (CSI) [12]. This method allows for highly accurate estimation over a wide frequency band. However, because the pilot signal is inserted at the end of the packet, the Doppler shift cannot be estimated until the entire packet is received, resulting in a delay. Other techniques for Doppler frequency estimation include using radar to evaluate the dynamic characteristics of a target and applying overlapping frequency domain equalization [13,14]. While these techniques can also achieve high accuracy, they have limitations, such as high computational complexity and a restricted range of Doppler frequencies that can be estimated. Recently, a method was proposed to estimate the Doppler shift using convolutional neural networks (CNNs) to analyze the spectrogram of the received signal in the time-frequency domain. Although this machine learning-based approach shows promise, its high computational complexity makes it challenging to apply in real-time systems with limited computational resources [10].

In high-mobility communication environments, quickly assessing the surrounding communication situation is critical, necessitating a novel method that reduces latency while maintaining estimation performance. To address this, we propose a novel estimation method for the maximum Doppler shift using decision feedback channel estimation (DFCE). The vast majority of modern wireless communication systems utilize packet-based transmission, with pilot-aided channel estimation (PCE) being a widely recognized method where known training symbols are inserted at the beginning of each packet [15]. In conventional methods, pilot signals are also placed at the end of the packet to improve estimation accuracy. However, this introduces significant latency as Doppler shifts cannot be estimated until the entire packet is received. To overcome this limitation, we propose leveraging an information signal within the packet to fulfill the role of the pilot signal traditionally inserted at the end. In fast-fading environments characterized by double selectivity, rapid channel variations can lead to significant errors in the channel state information (CSI) estimated by PCE and in the demodulated information signal. DFCE effectively mitigates these errors by using both pilot symbols and a replica signal. DFCE generates the replica

signal by remodulating the received signal, which has been corrected and demodulated using the pilot signal at the beginning of the packet. This high-accuracy replica signal can be treated as a known signal [16], thereby allowing it to replace the conventional pilot signal inserted at the end of the packet. The maximum Doppler shift is detected by analyzing phase changes in the CSI obtained from both the initial pilot and the replica signals. Since the proposed method eliminates the need to wait until the entire packet has been received, it effectively addresses the significant delay problem associated with conventional methods while maintaining high estimation accuracy.

The main contribution of this paper is the estimation of the maximum Doppler shift using the DFCE method, which can help reduce latency problems. As a reminder, the channel model is presented in Section 2. Section 3 describes the proposed method for estimating the Doppler shift using DFCE. Simulation results are discussed in Section 4 to evaluate the estimation accuracy and processing time. The conclusions are provided in Section 5.

## 2. System Model

This paper assumes an environment characterized by selective fading and Doppler shifts, which is one of the most common models for highly mobile communications and ensures adequate reliability [17].

### 2.1. Channel Model

This paper assumes a multipath and time-selective channel following the Jakes model [18]. We assume that the transmission channel consists of $L$ different paths; each path consists of a different delay time wave. In this case, the channel impulse response $h(t, \tau)$ can be represented as follows:

$$h(t, \tau) = \sum_{l=0}^{L-1} h_l(t)\delta(\tau - \tau_l) = \sum_{l=0}^{L-1} h_l(t)\delta\left(\tau - \frac{l}{W}\right), \tag{1}$$

where

$$L = \lfloor WT_m \rfloor + 1, \tag{2}$$

$L$ indicates the number of discrete paths, $h_l$ denotes the complex gain of each path, $\tau_l$ represents the delay time, $W$ indicates the bandwidth, $\lfloor \cdot \rfloor$ denotes the floor function, and $T_m$ represents the multipath spread. Here, $h_l(t)$ can be written as follows:

$$h_l(t) = \frac{g_l}{\sqrt{U}} \sum_{u=1}^{U} \exp[j(2\pi f_D t \cos \alpha_u + \phi_u)], \tag{3}$$

$g_l$ indicates the $l$-th path gain, $\alpha_u$ denotes the angle of arrival for the $u$-th wave, $\phi_u$ represents the initial phase of the $u$-th wave, and $f_D$ indicates the maximum Doppler shift. The sum of squared ensemble averages can be denoted as $\sum_{l=0}^{L-1} E[h_l^2] = 1$, where $E[\cdot]$ represents the ensemble average operation. The frequency response obtained by the Fourier transform of the impulse response is given by the following:

$$H(f, t) = \int_0^\infty h(\tau, t) \exp(-j2\pi f\tau) d\tau = \sum_{l=0}^{L-1} h_l(t) \exp(-j2\pi f\tau_l), \tag{4}$$

where $f$ indicates the carrier frequency. When $L$ is higher than or equal to 1, the channel results in frequency-selective fading, which can potentially cause degradation in communication quality [11,17].

### 2.2. Doppler Shift

The Doppler shift is the difference between the carrier frequency and received signal frequency due to the Doppler effect that occurs when the transmitter and receiver move

relative to each other. When an orthogonal frequency-division multiplexing (OFDM) signal is affected by the Doppler shift, inter-carrier interference (ICI) occurs, and the OFDM subcarriers lose their orthogonality, degrading communication performance significantly. When we set the initial phase $\varphi_n$, the phase $\varphi_{D_n}$ under the Doppler shift environment is as shown in (5), and the overall phase $\theta_n(t)$ is represented as in (6):

$$\varphi_{D_n} = \int_t 2\pi f_{D_n}(t)dt, \tag{5}$$

$$\theta_n(t) = 2\pi f_c \tau(t) - \varphi_{D_n}. \tag{6}$$

Using the above, the channel transfer function in (4) can be rewritten as follows:

$$H(f,t) = \sum_{l=0}^{L-1} h(t) \exp\{j\theta_n(t)\}. \tag{7}$$

$h_k$ is the $k$-th multipath channel response; it can be expressed using the standard deviation of the channel tap $\sigma_k$ and the sum of multiple elements following a complex Gaussian process with a unity variance $\vartheta_k(t)$ as follows:

$$h_k(t) = \sigma_k \vartheta_k(t). \tag{8}$$

The autocorrelation function of the channel taps is given by the following:

$$R_k(\tau) = E[h_k(t)h_k^*(t+\tau)]\delta(t-(t-\tau)) = \sigma_k J_0(2\pi f_D \tau), \tag{9}$$

where $J_0(\cdot)$ indicates the zeroth-order Bessel function. As a result, the Doppler power spectrum is expressed as follows:

$$D_k(f) = \int_{-\infty}^{\infty} R(\tau) \exp\left(-j2\pi f\tau\right)d\tau. \tag{10}$$

From (10), each channel is significantly distorted due to Doppler shifts in the frequency domain. In addition, when a Doppler shift occurs in a multipath environment, each path is affected by a different Doppler shift, resulting in a Doppler spread that spreads the frequency of the received signal. Large Doppler spreads cause rapid channel fluctuations and shorter coherence times. There is a relationship between the Doppler spread $B_d$ and the coherence time $T_c$ as follows:

$$T_c \propto \frac{1}{B_d}. \tag{11}$$

Observing (11), each channel is also significantly distorted due to Doppler shifts in the time domain. Therefore, the Doppler shift makes communication difficult in time and frequency domains.

## 3. Maximum Doppler Shifts Estimation

Double-selective fading, as introduced in the system model, is a tough issue in high-mobility communications, so techniques such as changing the modulation scheme—depending on the level of mobility—are effective [10]. This paper assumes that the user's mobility is constant.

### 3.1. Conventional Method

Conventional methods assume that the receiver moves at a constant speed around the transmitter. In addition, the moving speed of the receiver is discrete, and the best one can be selected from the assumed candidate moving speeds. This is used to perform Doppler frequency detection based on likelihood estimation by comparing the fluctuations of the channel state information in the packet with a threshold value. Figure 1 shows the structures of the packet used in the conventional methods. In the conventional method,

pilot signals are added at the first and last of each data packet, and the pilot signals sandwich each data packet. Therefore, CSI estimation is performed at the first and last of the packets. Then, by comparing the estimated CSI at the first and last of the packets, the variation in CSI is verified against a pre-set threshold value. The verification results are used to determine the most appropriate candidate for the receiver's movement speed. $\bar{h}_0(k)$ and $\bar{h}_{N-1}(k)$ represent the first and last estimated CSIs of the $k$-th packet, respectively. Based on these values, the variation of each packet, denoted as $\epsilon(k)$, is defined as follows:

$$\epsilon(k) = |\bar{h}_{N-1}(k) - \bar{h}_0(k)|^2. \tag{12}$$

In high-mobility environments, variations in the CSI are due to Doppler frequency and external noise. The metric $\epsilon(k)$ can be decomposed into two parts, namely, $\epsilon_c(k) \in \mathbb{R}$ due to the AWGN and $\epsilon_d(k) \in \mathbb{R}$ due to Doppler frequency.

$$\epsilon(k) = \epsilon_c(k) + \epsilon_d(k). \tag{13}$$

Even if the maximum Doppler frequency is constant, the channel variation value is different for each packet. Therefore, assuming that CSI variation values vary randomly like Gaussian random variables, the AWGN also follows a Gaussian distribution. So, both the probability density functions (PDF) of the variation values $\epsilon_d(k)$ and $\epsilon_c(k)$ can be expressed as exponential functions. When $P_{\text{PDF}}(\epsilon_c) \in \mathbb{R}$ and $P_{\text{PDF}}(\epsilon_d) \in \mathbb{R}$, which are the probability density functions of $\epsilon_c(k)$ and $\epsilon_d(k)$ respectively, these functions can be expressed as follows:

$$P_{PDF}(\epsilon_c) = k_c e^{-k_c \epsilon_c}, \tag{14}$$

$$P_{PDF}(\epsilon_d) = k_d e^{-k_d \epsilon_d}. \tag{15}$$

$k_c \in \mathbb{R}$ in (14) and $k_d \in \mathbb{R}$ in (15) are the inverses of the mean values of $\epsilon_c(k)$ and $epsilon_d(k)$, respectively. Since the metric is the sum of deviation and fluctuation values, such as in (13), the PDF of the metric, $P_{PDF}(\epsilon) \in \mathbb{R}$, is expressed as follows:

$$P_{PDF}(\epsilon) = \frac{k_c k_d}{k_d - k_c}(e^{-k_c \epsilon} - e^{-k_d \epsilon}), k_c \neq k_d. \tag{16}$$

As shown in (16), $P_{PDF}(\epsilon)$ is composed of two exponential functions. Therefore, once the PDFs for the two maximum Doppler frequencies are defined, the cumulative density function (CDF) and the complementary cumulative density function (CCDF) can be easily calculated. Let $v_1$ and $v_2$ be the candidate speeds of the receiver. However, assume that $v_1 > v_2$. If $\epsilon_0$ is the threshold value, the detection error performance can be expressed as $P_{CDF}^{v_2}(\epsilon_0)$ when the speed of the receiver is $v_2$. On the other hand, when the receiver speed is $v_1$, the detection error performance can be expressed as $P_{CCDF}^{v_1}(\epsilon_0)$. When the PDF is defined by (16), the CDF $P_{CDF}^{(v_i)}(\epsilon)$ is a monotonically increasing function with respect to $\epsilon$, and $P_{CCDF}^{(v_i)}(\epsilon)$ is a monotonically decreasing function. In other words, there is a trade-off between the two detection error performances with respect to the threshold. This means that there is only one optimal threshold value, which can be defined as follows:

$$P_{CCDF}^{v_1}(\epsilon_0) = P_{CDF}^{v_2}(\epsilon_0). \tag{17}$$

Thus, this conventional method derives a theoretical threshold by assuming that fluctuations are exponentially distributed. Therefore, the proposed detection can be implemented with a small computational effort, as the threshold is obtained by offline computation [12]. However, since the pilot signal is inserted at the last part of the packet, the Doppler shift cannot be detected until the packet is completely received. This means that this method has a critical latency.
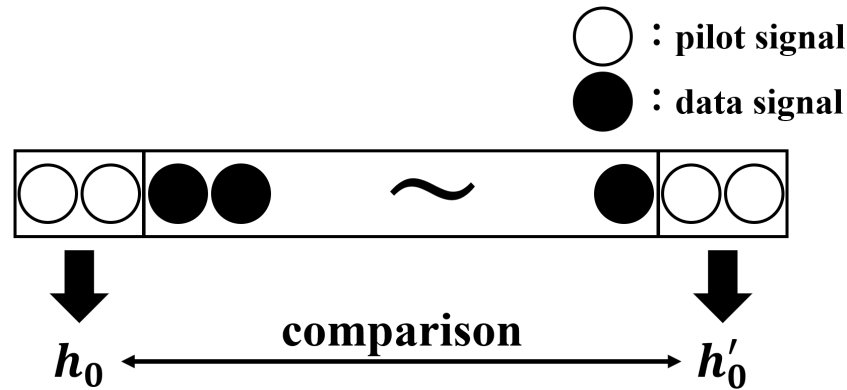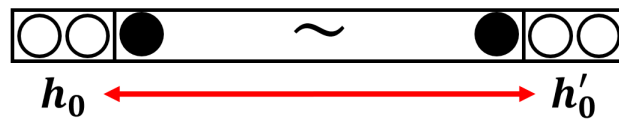
**Figure 1.** This diagram shows the transmitted packets used in the conventional methods.

### 3.2. Proposed Method

Figure 2 compares the structures of the packet used in the conventional and proposed methods. The proposed method aims to reduce the estimation time while maintaining accuracy compared to the conventional method by using DFCE.
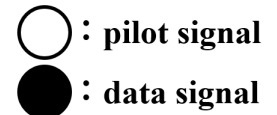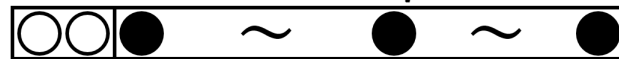


**Figure 2.** This diagram compares the transmitted packets used in the conventional and proposed methods.

#### 3.2.1. Decision Feedback Channel Estimation

Decision feedback channel estimation (DFCE) is an advanced technique aimed at enhancing the accuracy of channel estimation. A technique called PCE is often used to estimate the channel from pilot signals inserted at the beginning of communication packets. However, accurate estimation is difficult in high-speed fading environments due to the high channel fluctuations. Therefore, decision feedback channel estimation (DFCE) enables accurate channel estimation even under fast fading by re-evaluating the channel characteristics based on the corrected data symbols.

DFCE first performs channel estimation in a similar way to PCE. The channel response is estimated by the pilot signal inserted at the beginning of the data packet. If the transmitted signal is $S(k)$ and the received signal is $r(k)$, the following relationship holds:

$$r(k) = h(k)S(k) + n(k). \tag{18}$$

In (18), $h(k)$ denotes the channel response, and $n(k)$ denotes the noise, respectively. Therefore, the channel response $h_0$ of the pilot signal is as follows:

$$h_0(k) = \frac{r_0(k)}{S_0(k)} - \frac{n_0(k)}{S_0(k)}. \tag{19}$$

In (19), $n(k)$ is assumed to be AWGN and AWGN follows a Gaussian distribution. Therefore, by averaging multiple pilot signals, the noise effect can be reduced to ignore, and a highly accurate channel response can be obtained. In this case, the averaged pilot signal channel response $\bar{h}_0$ is expressed as follows:

$$\bar{h}_0 = \frac{\sum_{k=1}^{p} h_0(k)}{p}. \tag{20}$$

Assuming that there is little variation in the channel response within the same packet, the receiver and channel response can be used to estimate the transmitted signal. However, in high-mobility environments, the channel changes rapidly within the same packet. Therefore, the DFCE performs channel compensation using only a part of the data packet (up to the $\gamma$-th in this paper). Assuming that the compensation up to the $\gamma$-th is ideal, the information signal can be estimated with infinitely high accuracy. The estimated information signal obtained here is remodulated to obtain a replica signal. Since the demodulation of the information signal is assumed to be ideal, the replica signal $\hat{S}_\gamma$ can be assumed to be the same as the original data symbol, as follows:

$$S_\gamma = \hat{S}_\gamma. \tag{21}$$

Substituting the $\gamma$-th received signal and the replica signal into (18) gives the channel response $h_\gamma$ of the $\gamma$-th packet, which enables more accurate channel compensation after the $\gamma$-th packet as shown in Figure 3. Thus, by estimating the channel response in data packets, DFCE can cope with severe channel changes in a fast-fading environment.
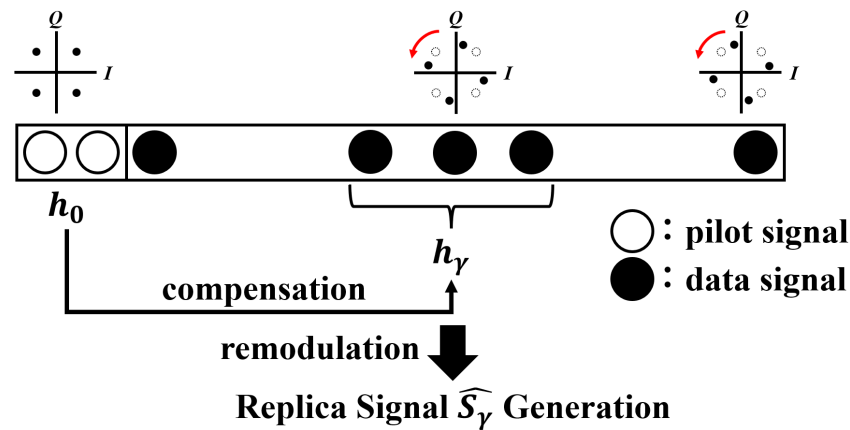


**Figure 3.** This diagram illustrates the principle of the DFCE.

3.2.2. Maximum Doppler Shift Estimation

The maximum Doppler shift is equivalent to the phase change in the channel response; therefore, the Doppler shift can be expressed as follows:

$$f_D = \frac{\arg \exp(\theta_\gamma - \theta_0)}{2\pi\Delta\tau} = \frac{\arg \Delta h}{2\pi\Delta\tau}. \tag{22}$$

$\Delta h$, the channel variation from the first pilot signal to the $\gamma$th data signal, is expressed as follows:

$$\Delta h = \frac{h_\gamma}{h_0} = \frac{h_\gamma S_\gamma}{h_0 S_\gamma}, \tag{23}$$

since the product of $h\gamma$ and $S_\gamma$ in (23) can be interpreted as the received signal itself, the fluctuation in the channel response, $\Delta h$, can be expressed as follows:

$$\Delta h = \frac{r_\gamma}{h_0 S_\gamma}. \tag{24}$$

From (21), the replica signal obtained by the DFCE can be considered equivalent to the original data symbol, so $\Delta h$ can be obtained as follows:

$$\Delta h = \frac{r_\gamma}{h_0 \hat{S}_\gamma}. \tag{25}$$

Therefore, from (24) and (22), $f_D$ is as follows:

$$f_D = \frac{1}{2\pi\Delta\tau}\left(\arg\frac{r_\gamma}{h_0 \hat{S}_n}\right). \tag{26}$$

**4. Numerical Result**

The simulation parameters used in this study are presented in Table 1. In our simulations, we assume a Rayleigh fading channel, with orthogonal frequency division multiplexing (OFDM) employed for both transmission and reception. The scenario assumes constant user movement, and we compare the accuracy of maximum Doppler shift estimation using both conventional and proposed methods, as well as their respective processing times. In OFDM systems, the pilot signal averaging channel estimation is generally used to identify the channel state information (CSI). In this case, large pilot symbols are required to obtain an accurate CSI. As a result, the total transmission rate is degraded due to the transmission of large pilot symbols. In this paper, two pilot symbols are used. The transmitted signals are subject to broadband channel propagation. Five path Rayleigh fadings have exponential shapes with path separation, $T_{path} = 140$ s. This case results in severe frequency selective fading. In this simulation, we focus on terrestrial systems. Consider a packet consisting of 64 subcarriers and 20 OFDM symbols, with the number of pilot symbols being $N_d = 18$), and the transmission rate is considered about 100 Ksymbols/s for individual subcarriers. Assuming the mobile unit travels at approximately 58 m/s (208 km/h) and operates at 5 GHz, the Doppler frequency is approximately $F_d = 966$ Hz. The Jakes correlation between two fading coefficients separated by t time samples is given by $J_0(2F_d T_s t)$, where Ts is the symbol period and $J_0$ is the zeroth-order Bessel function of the first kind. We assume that $T_s = 1/100{,}000 = 10$ μs, so $T_s F_d = 0.0096$. Therefore, the maximum Doppler frequency is assumed to range from 0 Hz to 1000 Hz.

**Table 1.** Simulation parameters.

| Parameter | Value |
|---|---|
| IFFT size | 64 |
| Number of pilot symbols | 2 |
| Number of subcarriers | 62 |
| Number of symbols | 20 |
| Length of guard interval | 16 |
| Modulation | BPSK |
| Bandwidth | 20 MHz |
| Number of paths | 5 |
| Doppler frequency | 0–1000 Hz |

*4.1. Optimization for DFCE*

Figure 4 shows the estimation accuracy results for the maximum Doppler shift as the parameter $\gamma$ varies, with an Eb/No of 20 dB in the proposed method. As indicated in Figure 4, increasing the value of $\gamma$ improves the estimation accuracy. This improvement

occurs because the Doppler shift's impact on the signal is minimized when the initial part of the packet is used. Also, Figure 5 shows the estimation time results for the maximum Doppler shift as the parameter $\gamma$ varies, with an Eb/No of 20 dB in the proposed method. As indicated in Figure 5, the more the parameter $\gamma$ increases, the longer it takes to estimate. This is believed to be because the data symbols targeted for replica signals generated using DFCE are located later in the packet, which increases the time required to receive them. However, while a higher $\gamma$ value enhances accuracy, it also increases the processing time, highlighting a trade-off between these two factors. In subsequent simulations, we selected $\gamma = 10$ to strike a balance between the accuracy and processing time.
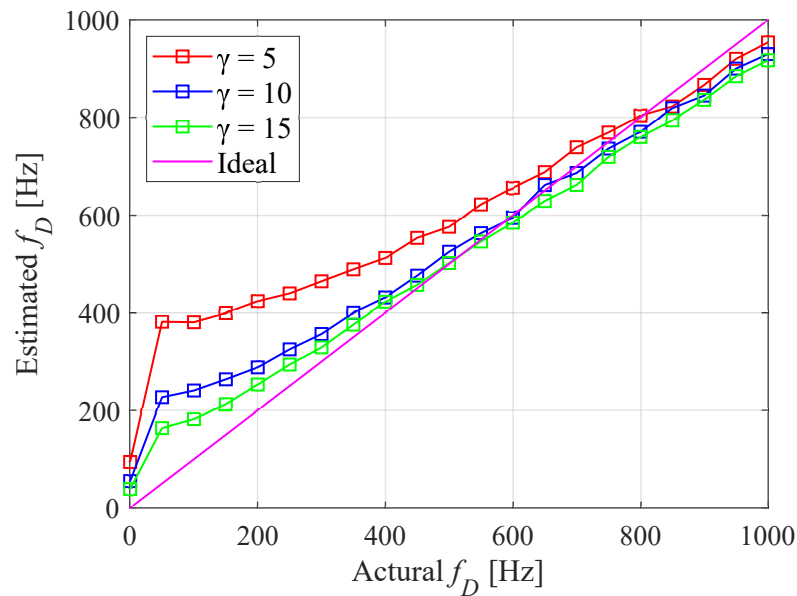


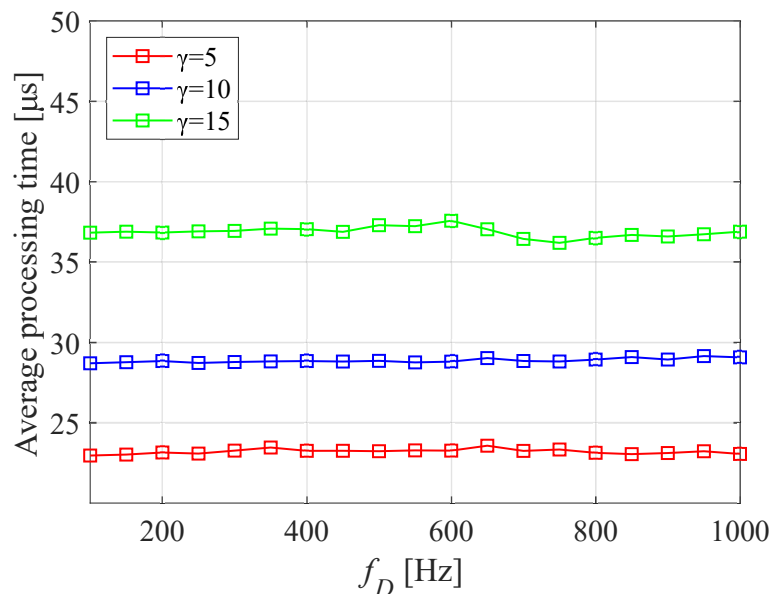**Figure 4.** Detection accuracy when varying the parameter $\gamma$.



**Figure 5.** Detection time when varying the parameter $\gamma$.

*4.2. Comparison Results*

Figures 6 and 7 illustrate the estimation results for the maximum Doppler shift using the conventional and proposed methods, respectively. From these figures, it is evident that estimation accuracy decreases as Eb/No decreases. Specifically, Figure 6 shows that

the conventional method struggles to provide accurate estimates at an Eb/No of 0 dB. Conversely, in environments where Eb/No exceeds 20 dB, both methods demonstrate high estimation accuracy.

A closer examination of Figure 6 reveals that the detection accuracy of the conventional method deteriorates when the maximum Doppler frequency exceeds 400 Hz, with an estimation error of approximately 50 Hz when the maximum Doppler frequency surpasses 800 Hz. In contrast, as shown in Figure 7, the proposed method can limit the estimation error to within 10 Hz when the maximum Doppler frequency is below 800 Hz, and within 50 Hz, even when the maximum Doppler frequency exceeds 800 Hz.
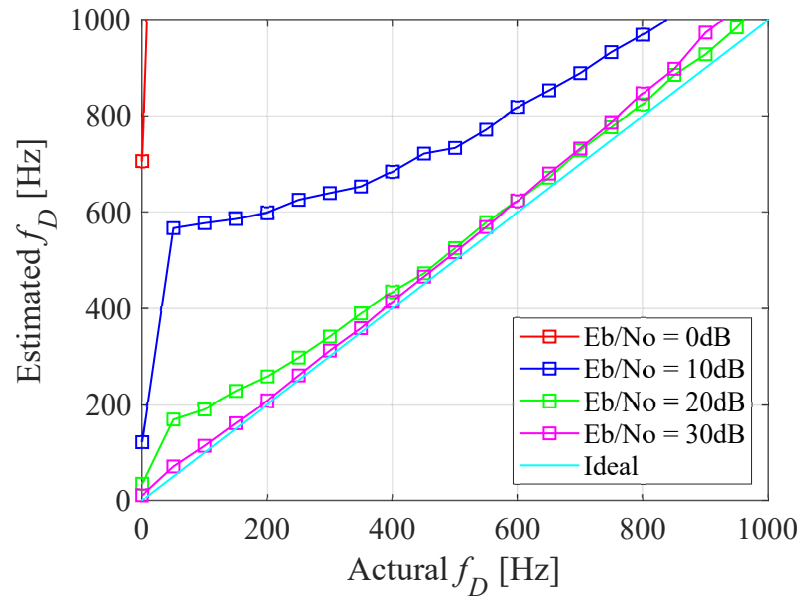


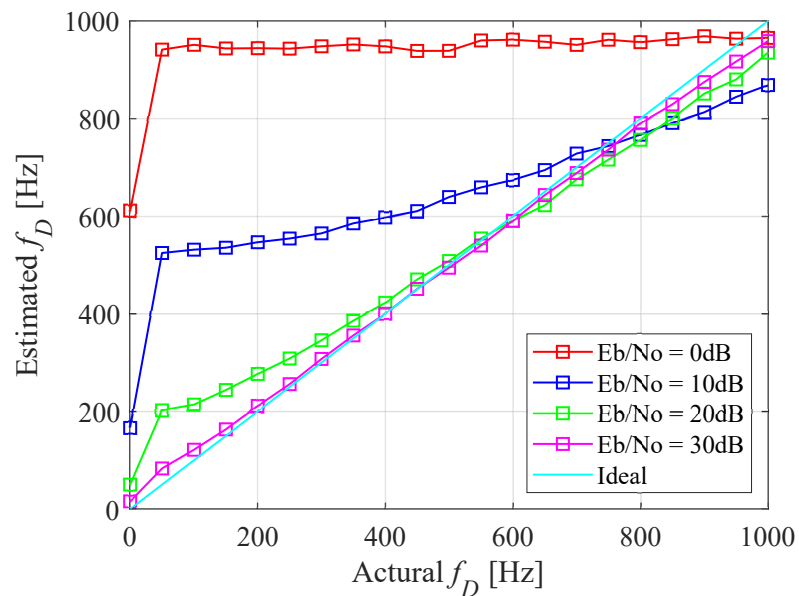**Figure 6.** Simulation results with the conventional method for various Eb/No values.



**Figure 7.** Simulation results with the proposed method for various Eb/No values.

### 4.3. Computational Complexity

Figure 8 compares the processing times between the proposed and conventional methods. The processing time for the conventional method is 3.79 µs, while the proposed method reduces this time to 2.96 µs. This demonstrates that the proposed method signif-

icantly decreases processing latency compared to the conventional method, making it a more efficient option for real-time applications.
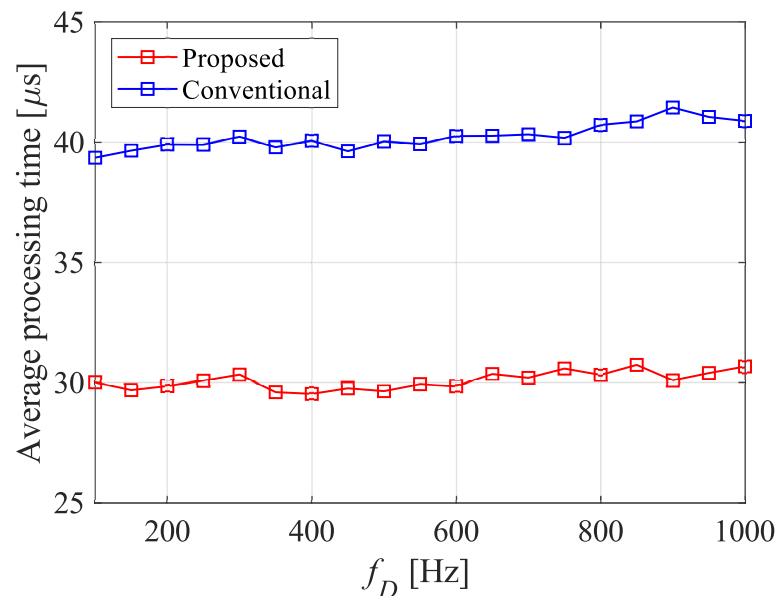


**Figure 8.** Simulation results of processing time differences.

## 5. Conclusions

Fast maximum Doppler frequency estimation plays an important role in enabling adaptive communication systems that can be applied beyond 5G and 6G networks. The purpose of this paper is to solve the latency problem in conventional methods. In this paper, we propose maximum Doppler shift estimation using DFCE to enable faster estimation. Using the DFCE eliminates the need to wait for the entire communication packet to be received by treating the data symbols as known signals and reducing the pilot signal. Throughout the simulations, processing time was reduced by 1.3 times. Furthermore, accuracy was improved compared to the conventional method. The proposed method also presents a trade-off between estimation accuracy and detection time. Therefore, the parameter $\gamma$, which is the target of the replica signal generated by the DFCE, is a very important parameter.

**Author Contributions:** Y.H. is the main author. H.H., R.T., K.T. and J.C. provided methodology, software, and constructive feedback on every part of the manuscript. C.-J.A. is the supervisor. All authors have read and agreed to the published version of the manuscript.

**Data Availability Statement:** Data are contained within the article.

## References

1. Muntadher, A.; Marwah, A.N.; Basheera, M.M.; Sadiq, H.A.; Mohammad, R.E.; Ahmed, B.; Nor, K.N.; Sadiq, M.S.; Khaled, A.U.; Fazirul, H. 6G Wireless Communications Networks: A Comprehensive Survey. *IEEE Access* **2021**, *9*, 148191–148243.
2. Lal, C.G. Applications of antenna arrays to mobile communications. I. Performance improvement, feasibility, and system considerations. *Proc. IEEE* **1997**, *85*, 1031–1060.
3. Mostafa, Z.C.; Shahjalal, M.; Shakil, A.; Yeong, M.J. 6G Wireless Communication Systems: Applications, Requirements, Technologies, Challenges, and Research Directions. *IEEE Open J. Commun. Soc.* **2020**, *1*, 957–975.
4. Henrik, M.; Ingo, V.; Andreas, L.; Bernhard, W. Mobility and Reliability in LTE-5G Dual Connectivity Scenarios. In Proceedings of the 2017 IEEE 86th Vehicular Technology Conference (VTC-Fall), Toronto, ON, Canada, 24–27 September 2017; pp. 1–4.

5. Noor-A-Rahim, M.; Liu, Z.; Lee, H.; Khyam, M.O.; He, J.; Pesch, D.; Moessner, K.; Saad, W.; Poor, H.V. 6G for vehicle-to-everything (V2X) communications: Enabling technologies, challenges, and opportunities. *Proc. IEEE* **2022**, *110*, 712–734. [CrossRef]

6. Chen, S.; Sun, S.; Kang, S. System integration of terrestrial mobile communication and satellite communication —the trends, challenges and key technologies in B5G and 6G. *China Commun.* **2020**, *17*, 156–171. [CrossRef]

7. Wei, Z.; Yuan, W.; Li, S.; Yuan, J.; Bharatula, G.; Hadani, R.; Hanzo, L. Orthogonal time-frequency space modulation: A promising next-generation waveform. *IEEE Wireless Commun.* **2021**, *28*, 136–144. [CrossRef]

8. Victor, M.B. Incorporating Spatial Modulation for Non-Coherent Massive MIMO with DPSK Schemes. *IEEE Wirel. Commun. Lett.* **2024**, *13*, 2527–2530.

9. Shun, K.; Takashi, A.; Koya, W.; Masato, K.; Ahn, C.-J. Adaptive switching method with AMC and FSS. In Proceedings of the 2018 26th International Conference on Software, Telecommunications and Computer Networks (SoftCOM), Split, Croatia, 13–15 September 2018; pp. 1–6.

10. Shun, K.; Maruta, K.; Feng, Y.; Ahn, C.-J.; Tarokh, V. CNN-based joint SNR and Doppler shift classification using spectrogram images for adaptive modulation and coding. *IEEE Trans. Commun.* **2021**, *69*, 5152–5167.

11. Tamura, K.; Kojima, S.; Trinh, P.V.; Sugiura, S.; Ahn, C.-J. Joint SNR and rician K-factor estimation using multimodal network over mobile fading channels. *IEEE Trans. Mach. Learn. Commun. Netw.* **2024**, *2*, 766–779. [CrossRef]

12. Denno, S.; Hotta, K.; Hou, Y. User mobility estimation through maximum Doppler frequency detection. In Proceedings of the 2021 15th International Conference on Signal Processing and Communication Systems (ICSPCS), Sydney, Australia, 13–15 December 2021; pp. 1–5.

13. Xingjian, D.; Shiqian, C.; Guanpei, X.; Zhike, P.; Wenming, Z.; Guang, M. Doppler Frequency Estimation by Parameterized Time-Frequency Transform and Phase Compensation Technique. *IEEE Sens. J.* **2018**, *18*, 3734–3744.

14. Kohei, H.; Satoshi, D.; Kazuoki, I.; Takashi, O.; Yuji, A. Doppler Frequency Estimation using Overlap Frequency Domain Equalization. In Proceedings of the 2018 21st International Symposium on Wireless Personal Multimedia Communications (WPMC), Chiang Rai, Thailand, 25–28 November 2018; pp. 256–261.

15. Takaki, O.; Shun, K.; Kazuki, M.; Ahn, C.-J. Neural Network based Channel Identification and Compensation. In Proceedings of the 2018 18th International Symposium on Communications and Information Technologies (ISCIT), Bangkok, Thailand, 26–29 September 2018; pp. 349–354.

16. He, H.; Wang, J.-H.; Kojima, S.; Maruta, K.; Ahn, C.-J. Regression CNN based fast fading channel tracking using decision feedback channel estimation. *J. Signal Process.* **2023**, *27*, 49–57. [CrossRef]

17. Kojima, S.; Maruta, K.; Ahn, C.-J. Adaptive modulation and coding using neural network based SNR estimation. *IEEE Access* **2019**, *7*, 183545–183553. [CrossRef]

18. Jakes, W.C. *Microwave Mobile Communication*; IEEE Press: Piscataway, NJ, USA, 1994.